

AperTO - Archivio Istituzionale Open Access dell'Università di Torino

Dextran-shelled oxygen-loaded nanodroplets reestablish a normoxia-like pro-angiogenic phenotype and behavior in hypoxic human dermal microvascular endothelium

This is the author's manuscript

Original Citation:

Availability:

This version is available <http://hdl.handle.net/2318/1532885> since 2016-11-28T09:58:48Z

Published version:

DOI:10.1016/j.taap.2015.08.005

Terms of use:

Open Access

Anyone can freely access the full text of works made available as "Open Access". Works made available under a Creative Commons license can be used according to the terms and conditions of said license. Use of all other works requires consent of the right holder (author or publisher) if not exempted from copyright protection by the applicable law.

(Article begins on next page)

This Accepted Author Manuscript (AAM) is copyrighted and published by Elsevier. It is posted here by agreement between Elsevier and the University of Turin. Changes resulting from the publishing process - such as editing, corrections, structural formatting, and other quality control mechanisms - may not be reflected in this version of the text. The definitive version of the text was subsequently published in TOXICOLOGY AND APPLIED PHARMACOLOGY, 288 (3), 2015, 10.1016/j.taap.2015.08.005.

You may download, copy and otherwise use the AAM for non-commercial purposes provided that your license is limited by the following restrictions:

- (1) You may use this AAM for non-commercial purposes only under the terms of the CC-BY-NC-ND license.
- (2) The integrity of the work and identification of the author, copyright owner, and publisher must be preserved in any copy.
- (3) You must attribute this AAM in the following format: Creative Commons BY-NC-ND license (<http://creativecommons.org/licenses/by-nc-nd/4.0/deed.en>), 10.1016/j.taap.2015.08.005

The publisher's version is available at:

<http://linkinghub.elsevier.com/retrieve/pii/S0041008X15300570>

When citing, please refer to the published version.

Link to this full text:

<http://hdl.handle.net/2318/1532885>

Dextran-shelled oxygen-loaded nanodroplets reestablish a normoxia-like pro-angiogenic phenotype and behavior in hypoxic human dermal microvascular endothelium.

Running head: Oxygen nanodroplets in hypoxic dermal endothelium.

Nicoletta Basilico^a, Chiara Magnetto^b, Sarah D'Alessandro^c, Alice Panariti^d, Ilaria Rivolta^d,
Tullio Genova^e, Amina Khadjavi^f, Giulia Rossana Gulino^g, Monica Argenziano^h, Marco
Soster^h, Roberta Cavalli^h, Giuliana Giribaldi^g, Caterina Guiot^f, Mauro Prato^{f,*}

^a *Dipartimento di Scienze Biomediche, Chirurgiche e Odontoiatriche, Università di Milano,
via Pascal 36 – 20133, Milano, Italy*

^b *Istituto Nazionale di Ricerca Metrologica (INRIM), Strada delle Cacce, 91 – 10135,
Torino, Italy*

^c *Dipartimento di Scienze Farmacologiche e Biomolecolari, Università di Milano, via Pascal
36 – 20133, Milano, Italy*

^d *Dipartimento di Scienze della Salute, Università di Milano Bicocca, Via Cadore 48 –
20900, Monza, Italy*

^e *Dipartimento di Scienze della Vita e Biologia dei Sistemi, Via Accademia Albertina 13,
10123, Torino, Italy*

^f *Dipartimento di Neuroscienze, Università di Torino, Corso Raffaello 30 – 10125, Torino,
Italy*

^g *Dipartimento di Oncologia, Università di Torino, Via Santena 5 bis – 10126, Torino, Italy*

^h *Dipartimento di Scienza e Tecnologia del Farmaco, Università di Torino, Via Giuria, 9 –
10125, Torino, Italy*

* corresponding author: Dr. Mauro Prato, Dipartimento di Neuroscienze, Università di
Torino, Corso Raffaello 30, 10125 Torino, Italy; Phone: +39-011-670-8198; Fax:+39-011-
670-8174; e-mail: mauro.prato@unito.it

26 E-mail addresses:
27 Nicoletta Basilico: nicoletta.basilico@unimi.it
28 Chiara Magnetto: c.magnetto@inrim.it
29 Sarah D'Alessandro: sarah.dalessandro@unimi.it
30 Alice Panariti: alice.panariti@mail.mcgill.ca
31 Ilaria Rivolta: ilaria.rivolta@unimib.it
32 Tullio Genova: tullio.genova@unito.it
33 Amina Khadjavi: amina.khadjavi@unito.it
34 Giulia Rossana Gulino: giuliarossana.gulino@unito.it
35 Monica Argenziano: monica.argenziano@unito.it
36 Marco Soster: marco.soster@unito.it
37 Roberta Cavalli: roberta.cavalli@unito.it
38 Giuliana Giribaldi: giuliana.giribaldi@unito.it
39 Caterina Guiot: caterina.guiot@unito.it
40 Mauro Prato: mauro.prato@unito.it

41

42 *Funding sources:* The work was funded by Compagnia di San Paolo (Ateneo-San Paolo 2011
43 ORTO11CE8R grant to CG and MP) and Università degli Studi di Torino (ex-60% 2013
44 intramural funds to GG and MP). MP holds a professorship granted by Università degli Studi
45 di Torino and Azienda Sanitaria Locale-19 (ASL-19). AK and MP are funded by a
46 partnership grant from the European Community and the Italian Ministry of Instruction,
47 University, and Research (CHIC grant no. 600841). NB and SDA research is supported by
48 the Italian Ministry of Instruction, University, and Research (PRIN 2013 grant).

49

50 *Conflict of interest disclosure:* Roberta Cavalli, Caterina Guiot and Mauro Prato have a
51 patent no. WO2015/028901 A1 (A nanostructure for the vehiculation of gas and/or active
52 ingredients and/or contrast agents and use thereof) issued. The other authors have nothing to
53 disclose.

54

Abstract

In chronic wounds, hypoxia seriously undermines tissue repair processes by altering the balances between pro-angiogenic proteolytic enzymes (matrix metalloproteinases, MMPs) and their inhibitors (tissue inhibitors of metalloproteinases, TIMPs) released from surrounding cells. Recently, we have shown that in human monocytes hypoxia reduces MMP-9 and increases TIMP-1 without affecting TIMP-2 secretion, whereas in human keratinocytes it reduces MMP-2, MMP-9, and TIMP-2, without affecting TIMP-1 release. Provided that the phenotype of the cellular environment is better understood, chronic wounds might be targeted by new oxygenating compounds such as chitosan- or dextran-shelled and 2H,3H-decafluoropentane-cored oxygen-loaded nanodroplets (OLNs). Here, we investigated the effects of hypoxia and dextran-shelled OLN on the pro-angiogenic phenotype and behavior of human dermal microvascular endothelium (HMEC-1 cell line), another cell population playing key roles during wound healing. Normoxic HMEC-1 constitutively released MMP-2, TIMP-1 and TIMP-2 proteins, but not MMP-9. Hypoxia enhanced MMP-2 and reduced TIMP-1 secretion, without affecting TIMP-2 levels, and compromised cell ability to migrate and invade the extracellular matrix. When taken up by HMEC-1, nontoxic OLN abrogated the effects of hypoxia, restoring normoxic MMP/TIMP levels and promoting cell migration, matrix invasion, and formation of microvessels. These effects were specifically dependent on time-sustained oxygen diffusion from OLN core, since they were not achieved by oxygen-free nanodroplets or oxygen-saturated solution. Collectively, these data provide new information on the effects of hypoxia on dermal endothelium and support the hypothesis that OLN might be used as effective adjuvant tools to promote chronic wound healing processes.

Keywords: oxygen; nanodroplet; matrix metalloproteinase (MMP); tissue inhibitor of metalloproteinase (TIMP); human microvascular endothelial cell (HMEC); skin.

Introduction

After injury, skin integrity must be restored promptly to reestablish the homeostatic mechanisms, minimize fluid loss, and prevent infection [Greaves et al., 2013]. This is achieved through wound healing, a complex biological process where multiple pathways are simultaneously activated to induce tissue repair and regeneration. Traditionally, acute wound healing is defined as a complex multi-step and multi-cellular process, distinguished in four phases involving different cell types: i) hemostasis, involving platelets; ii) inflammation, involving neutrophils, monocytes, and macrophages; iii) proliferation, involving keratinocytes, endothelial cells, and fibroblasts; and iv) matrix remodeling, involving keratinocytes, myofibroblasts, and endothelial cells. [Diegelmann et al., 2004]. In particular, during the third and fourth phases, the endothelium plays a pivotal role, since wound microvasculature is rebuilt through angiogenesis to restore the supply of oxygen, blood constituents and nutrients to the regenerating tissue, helping to promote fibroplasia and prevent sustained tissue hypoxia [Eming et al., 2014]. Notably, oxygen represents a key regulator of normal wound healing since it is required for collagen deposition, epithelialization, fibroplasia, angiogenesis, and resistance to infection [Castilla et al., 2012; Sen, 2009]. Once complete, these processes must be shut down in a precise order to prevent exaggerated or delayed responses.

In some cases, the combination of systemic (e.g. diabetes, vascular insufficiency, or ageing) or localized (e.g. bacterial infections and dysregulated proteolysis) factors produce persistent pathological inflammation resulting in chronic wound formation [Diegelmann et al., 2004]. A chronic wound is defined as a break in skin epithelial continuity lasting more than 42 days. Its prevalence varies with age, ranging approximately from 1% in the adult population to 3–5% in >65 year-old subjects [Greaves et al., 2013]. Approximately 7 million patients are

affected by chronic wounds in the United States, and an estimated \$25 billion dollars is spent annually on the treatment of these wounds [Castilla et al., 2012].

A typical feature of chronic wounds is unbalanced proteolytic activity, which overwhelms tissue protective mechanisms [Diegelmann et al., 2004; Pepper, 2001]. Within chronic wounds, activated cells such as endothelial, epithelial, and immune cells display increased production of proteases, including cathepsin G, urokinase and neutrophil elastase [Greaves et al., 2013]. Furthermore, pro-inflammatory cytokines strongly induce the production of matrix metalloproteinases (MMPs) and down-regulate the levels of tissue inhibitors of metalloproteinases (TIMPs), thereby creating an environment with unbalanced MMP/TIMP ratios [Diegelmann et al., 2004; Pepper, 2001]. Consequently, wound repair mediators become targets of proteases, and the resultant matrix degradation contributes to the delay in re-epithelialization, fibroplasia and angiogenesis [Pepper, 2001; Wells et al., 2015]. However, the effects of hypoxia on the secretion of MMPs and TIMPs by the cellular environment of the wound are dramatically different depending on the considered cell type. Therefore, it is extremely important to assess carefully the effects of hypoxia on each single cell population participating to the wound healing process, from monocytes and keratinocytes to endothelial cells and fibroblasts. In a couple of recent works published by our group hypoxia was shown to reduce MMP-9 and increase TIMP-1 without affecting TIMP-2 secretion by human monocytes [Gulino et al., 2015], whereas in human keratinocytes hypoxia was shown to reduce MMP-2, MMP-9, and TIMP-2 secretion without changing TIMP-1 levels [Khadjavi et al., 2015]. On the other hand, the effects of hypoxia on the secretion of gelatinases and their inhibitors by dermal microvascular endothelium still needed further investigation.

Provided the phenotype of the cellular environment at the milieu of the wound is better understood, new therapeutic approaches addressing hypoxia might help to face chronic

131 wounds. For this reason, the major role played by oxygen in essential wound healing
132 processes has attracted considerable clinical interest and yielded compelling data [Sen, 2009].
133 Additionally, scientific studies targeting the signaling pathways underlying oxygen response
134 within the milieu of the wound tissue are helping to better understand the biochemical
135 pathways involved in hypoxia sensing/response systems. This appears extremely crucial in
136 order to exploit new oxygenating treatments targeting hypoxia-response mechanisms within
137 the healing tissue, thus making them useful in the clinical management of chronic wounds.
138 So far, hyperbaric oxygen therapy remains a well-established, adjunctive treatment for
139 diabetic lower extremity wounds, when refractory to standard care practices [Sen, 2009].
140 However, hyperbaric oxygen therapy is expensive and uncomfortable. Moreover, further
141 rigorous randomized trials are needed to properly validate the outcomes of hyperbaric oxygen
142 therapy on chronic wounds associated with other pathologies (arterial ulcers, pressure ulcers,
143 and venous ulcers). Topical oxygen therapy, based on an O₂ gas emulsion applied to the
144 superficial wound tissue, represents another promising approach to enhance the oxygenation
145 of wounded tissues [Sen, 2009]. Major advantages of topical oxygen therapy appear to be its
146 independence of the wound microcirculation, its lower cost with respect to systemic oxygen
147 therapy, lower risks of oxygen toxicity, and its relative simplicity of handling and application.
148 In this context, intensive research is being pursued to develop new carriers able to release
149 therapeutically significant amounts of oxygen to tissues in an effective and time-sustained
150 manner, such as hemoglobin- or perfluorocarbon-based systems [Cabrales et al., 2013;
151 Schroeter et al., 2010]. Among the options currently under investigation, perfluoropentane
152 (PFP)-based oxygen-loaded nanobubbles have been proposed as efficient and biocompatible
153 ultrasound (US)-responsive tools for oxygen delivery [Cavalli et al., 2009a; Cavalli et al.,
154 2009b]. Furthermore, oxygen-loaded nanodroplets (OLNs), constituted by 2H,3H-
155 decafluoropentane (DFP) as core fluorocarbon and dextran or chitosan as shell

polysaccharides, have been recently developed, characterized, and patented by our group as innovative and nonconventional platforms of oxygen nanocarriers, available in formulations suitable for topical treatment of dermal tissues [Magnetto et al., 2014; Prato et al., 2015]. Intriguingly, while keeping all the advantages of nanobubbles, OLN_s display higher stability and effectiveness in oxygen storage and release, lower manufacturing costs and ease of scale-up. Encouragingly, chitosan-shelled OLN_s proved effective in counteracting the dysregulating effects of hypoxia on secretion of gelatinases and TIMPs by human keratinocytes [Khadjavi et al., 2015], whereas dextran-shelled OLN_s abrogated hypoxia-dependent alteration of MMP-9/TIMP-1 balances in human monocytes [Gulino et al., 2015]. To go beyond the current knowledge on MMP/TIMP dysregulation in the different cell populations within the milieu of chronic wounds and expand the available evidence on OLN effectiveness, in the present work we explored the effects of hypoxia and OLN_s on the pro-angiogenic phenotype and behavior of human dermal endothelium. To this purpose, a human dermal microvascular endothelial cell line (HMEC-1) was cultured *in vitro* both in normoxic and hypoxic conditions, in the presence or absence of dextran-shelled OLN_s. Then, cells were challenged for their viability, proteolytic phenotype (secretion of gelatinases and their inhibitors), and wound healing abilities [migration, invasion of the extracellular matrix (ECM), and formation of microvessel-like structures].

Methods

Materials

All materials were from Sigma-Aldrich, St Louis, MO, aside from those listed below. Sterile plastics were from Costar, Cambridge, UK; MCDB 131 medium was from Invitrogen, Carlsbad, CA; foetal calf serum was from HyClone, South Logan, UT; epidermal growth factor was from PeproTech, Rocky Hill, NJ; Cultrex was from Trevigen, Gaithersburg, MD; LDH Cytotoxicity Assay kit was from Biovision, Milpitas, CA; enzyme-linked immunosorbent assay (ELISA) kit for human MMP-2 was from Abnova, Taipei City, Taiwan; ELISA kits for human MMP-9, TIMP-1 and TIMP-2 were from RayBiotech, Norcross, GA; electrophoresis reagents and computerized densitometer Geldoc were from Bio-rad Laboratories, Hercules, CA; Synergy Synergy 4 microplate reader was from Bio-Tek Instruments, Winooski, VT; recombinant proMMP-9 and MMP-9 were produced and kindly gifted by Prof. Ghislain Opdenakker and Prof. Philippe Van den Steen; ethanol (96%) was obtained from Carlo Erba (Milan, Italy); culture implants for wound healing assay were from Ibidi GmbH (Planegg/Martinsried, Germany); Epikuron 200® (soya phosphatidylcholine 95%) was from Degussa (Hamburg, Germany); palmitic acid, DFP, dextran sodium salt (100 kDa), and polyvinylpyrrolidone were from Fluka (Buchs, Switzerland); ultrapure water was obtained using a 1-800 Millipore system (Molsheim, France); Ultra-Turrax SG215 homogenizer was from IKA (Staufen, Germany); Delsa Nano C analyzer was from Beckman Coulter (Brea, CA); Philips CM10 instrument was from Philips (Eindhoven, The Netherlands); XDS-3FL microscope was from Optika (Ponteranica, Italy); ECLIPSE Ti inverted microscope was from Nikon (Amsterdam, The Netherlands).

Dextran-shelled nanodroplet preparation and characterization

OLNs, oxygen-free nanodroplets (OFNs), and oxygen-saturated solution (OSS) were prepared as previously described [Prato et al., 2015]. Briefly, 1.5 ml DFP, 0.5 ml polyvinylpyrrolidone and 1.8 ml Epikuron® 200 (solved in 1% w/v ethanol and 0.3 % w/v palmitic acid solution) were homogenized in 30 ml phosphate-buffered saline (PBS) solution (pH 7.4) for 2 min at 24000 rpm by using Ultra-Turrax SG215 homogenizer. For OLN, the solution was saturated with O₂ for 2 min. Finally, 1.5 ml dextran or fluorescein isothiocyanate (FITC)-labeled dextran solution was added drop-wise whilst the mixture was homogenized at 13000 rpm for 2 min. For OFN and OSS PBS formulations, OLN preparation protocol was applied omitting O₂ or dextran/DFP addition, respectively. Immediately after manufacturing, nanodroplets were sterilized through ultraviolet (UV)-C ray exposure for 20 min and characterized for: morphology and shell thickness, by optical and transmitting electron microscopy; size, particle size distribution, polydispersity index and zeta potential, by dynamic light scattering; refractive index by polarizing microscopy; viscosity and shell shear modulus by rheometry; and oxygen content (before and after UV-C sterilization) through a chemical assay as previously described [Magnetto et al., 2014;Prato et al., 2015].

Cell cultures

A long-term cell line of dermal microvascular endothelial cells (HMEC-1) immortalized by SV 40 large T antigen [Ades et al., 1992] was kindly provided by the Center for Disease Control, Atlanta, GA. Cells were maintained in MCDB 131 medium supplemented with 10% foetal calf serum, 10 ng/ml of epidermal growth factor, 1 µg/ml of hydrocortisone, 2mM glutamine, 100 units/ml of penicillin, 100 µg/ml of streptomycin and 20 mM Hepes buffer, pH7.4. Before the experiments, HMEC-1 were seeded at 10⁵ cells/0.5 ml per well in 24-well flat bottom tissue culture clusters and incubated in a humidified CO₂/air-incubator at 37°C in complete medium. After overnight incubation to allow cells adhesion, HMEC-1 were treated

for 24 h with/without 10% v/v OLN_s, OFN_s, and OSS, either in normoxic (20% O₂) or hypoxic (1% O₂) conditions. At the end of each treatment, cell supernatants were collected and used for the following analyses.

Evaluation of OLN uptake by HMEC-1

HMEC-1 were plated in 24-well plates on glass coverslips and incubated in complete medium for 24 h with/without 10% v/v FITC-labeled OLN_s in a humidified CO₂/air-incubator at 37°C both in normoxic and hypoxic conditions. After 4',6-diamidino-2-phenylindole (DAPI) staining to visualize cells nuclei, fluorescence images were acquired by a LSM710 inverted confocal laser scanning microscope equipped with a Plan-Neofluar 63×1.4 oil objective, that allowed a field view of at least 5 cells. Wavelength of 488 nm was used to detect OLN_s, and of 460 nm to detect the labeled nuclei. The acquisition time was 400 ms.

Cytotoxicity studies

The potential cytotoxic effect of OLN and control formulations was measured as the release of lactate dehydrogenase (LDH) from HMEC-1 into the extracellular medium using the LDH Cytotoxicity Assay kit following the manufacturer's instructions. LDH was measured both in the extracellular medium and in the cells pellet. Briefly, cells were incubated for 24 h with/without 10% v/v OLN_s, OFN_s or OSS, either in normoxic (20 % O₂) or hypoxic (1 % O₂) conditions, in a humidified CO₂/air-incubator at 37°C. Then, cell supernatants were collected and centrifuged at 13000g for 2 min. Cells were washed with PBS and resuspended in 0.5 ml of Triton X100 (2% final concentration) to lyse cells. One hundred microliters of this solution or 100 microliters of supernatant was mixed with 100 microliters of LDH reaction mix, containing the LDH substrate, and incubated for 10 min at room temperature in

the dark. Absorbance was then read at 450 nm with a reference wavelength of 650 nm using Synergy 4 microplate reader.

Cell viability studies

Cell viability was evaluated using 3-(4,5-dimethylthiazol-2-yl)-2,5-diphenyltetrazolium bromide (MTT) assay. HMEC-1 were incubated in complete medium overnight to allow the cells to adhere and then treated for 24 h with/without 10% v/v OLN_s, OFN_s or OSS, either in normoxic (20 % O₂) or hypoxic (1 % O₂) conditions, in a humidified CO₂/air-incubator at 37°C in serum free medium. Thereafter, 20 µL of 5 mg/mL MTT in PBS were added to cells for 3 additional hours at 37 °C in the dark. The plates were then centrifuged, the supernatants discarded and the dark blue formazan crystals dissolved using 100 µL of lysis buffer containing 20 % (w/v) sodium dodecylsulfate, 40 % N,N-dimethylformamide (pH 4.7 in 80 % acetic acid). The plates were then read on Synergy 4 microplate reader at a test wavelength of 550 nm and at a reference wavelength of 650 nm.

Measurement of MMP-2, MMP-9, TIMP-1, and TIMP-2 production

HMEC-1 were incubated overnight in complete medium and then treated for 24 h with/without 10% v/v OLN_s, OFN_s or OSS, either in normoxic (20 % O₂) or hypoxic (1 % O₂) conditions, in a humidified CO₂/air-incubator at 37°C in serum-free medium. Thereafter, cell supernatants were collected, and the levels of MMP-2, MMP-9, TIMP-1, and TIMP-2 were assayed in 100 µl of HMEC-1 supernatants by specific ELISA. Standard calibration curves were generated with rhMMP-2, rhMMP-9, rhTIMP-1, and rhTIMP-2, according to the manufacturer's instructions. Of note, ELISA kits could not distinguish between latent and active forms of MMP-2 and MMP-9. For this reason, a complementary analysis by gelatin zymography was performed, as described in the following paragraph.

276

277 *Measurement of the levels of latent and active forms of gelatinases in cell supernatants*

278 The levels of latent and active forms of gelatinases were evaluated by gelatin zymography in
279 the cell supernatants as previously described [D'Alessandro et al., 2013]. Briefly, HMEC-1
280 were incubated overnight in complete medium and then treated for 24 h with/without 10%
281 v/v OLN_s, OFN_s or OSS, either in normoxic (20 % O₂) or hypoxic (1 % O₂) conditions, in a
282 humidified CO₂/air-incubator at 37°C in serum-free medium. Thereafter, 15 µl cell
283 supernatants/lane were loaded on 8% polyacrylamide gels containing 0.1% gelatin under non-
284 denaturing and non-reducing conditions. Following electrophoresis, gels were washed at
285 room temperature for 2 h in milliQ water containing 2.5% (v/v) Triton-X100 and incubated
286 for 18 h at 37°C in a collagenase buffer containing (mM): NaCl, 200; Tris, 50; CaCl₂, 10; and
287 0.018% (v/v) Brij 35, pH 7.5, with or without 5 mM ethylenediaminetetraacetic acid to
288 exclude aspecific bands. At the end of the incubation, the gels were stained for 15 min with
289 Coomassie blue (0.5% Coomassie blue in methanol/acetic acid/water at a ratio of 3:1:6). The
290 gels were destained in milliQ water. Densitometric analysis of the bands, reflecting the total
291 levels of latent and active forms of gelatinases, was performed using a computerized
292 densitometer.

293

294 *In vitro wound healing assay*

295 *In vitro* wound healing assay was performed on HMEC-1 cells using Ibidi's culture inserts
296 according to the manufacturer's instructions. One culture insert per well was placed in a 24-
297 well plate. Then, 70 µl from a suspension of 5x10⁵ cells/ml HMEC-1 cells were plated in
298 each chamber of Ibidi's culture inserts with cell growth medium. After 24 h, culture inserts
299 were detached resulting in two confluent monolayers, divided by a space (scratch) of 500 µm.
300 Thereafter, cells were washed with PBS and incubated in fresh medium for 8 h in the

presence or absence of 10% v/v OLN_s or OFN_s, either in normoxic or hypoxic conditions. For each condition, at least two different culture inserts were employed. At the end of the observational period, scratch images were taken using a Nikon Ti-e eclipse microscope. Scratches were also measured and normalized with a time 0 scratch (500 μm).

Microvessel-like structures formation

HMEC-1 were evaluated for the ability to spontaneously migrate and self-organize in microvessel-like structures when cultured on a basal membrane surface [Prato et al., 2011]. Cells were seeded (1×10^5 cells/well) in a 96-well plate previously covered with solidified Cultrex (50 μ/well), a growth factor-free basement membrane extract from murine Engelbreth-Holm-Swarm tumor. After 2 h of incubation in the presence or absence of 10% v/v OLN_s, each well was evaluated by optical microscopy. The formation of microvessel-like structures was measured as the number of crosses between microvessel-like structures counted in five randomly selected fields by two independent observers.

Statistical analysis.

For each set of experiments, data are shown as means + SEM (LDH, MTT, densitometry, ELISA, and Cultrex assay results) or as a representative image (confocal microscopy and gelatin zymography results) of at least three independent experiments with similar results. All data were analyzed by a one-way analysis of variance (ANOVA) followed by Tukey's post-hoc test (software: SPSS 16.0 for Windows, SPSS Inc., Chicago, IL) or by Student's *t* test.

Results

Characterization of dextran OLN preparations

Before use, all dextran-shelled OLN preparations were meticulously characterized for physico-chemical parameters. Results were always in line with published data [Prato et al., 2015]: OLN_s displayed spherical shapes, 590 nm average diameters, −25 mV zeta potential, 1.33 as refractive index value, 1.59 e-3 Pa·s as viscosity value, and 5.43 e-2 mPa as shear modulus value, calculated at a shear rate value of 150 s⁻¹. OLN_s also showed a good oxygen-storing capacity of 0.40 mg/ml of oxygen either before or after 20-min UV-C sterilization, and such an oxygen amount was comparable with that of OSS. Furthermore, all nanodroplet preparations proved to be stable over time, as confirmed by long-term checking of these parameters.

OLN uptake by human dermal microvascular endothelial cells

Confocal microscopy analysis was performed to determine whether OLN_s were internalized by endothelial cells. HMEC-1 were incubated with 10% v/v FITC-labeled dextran-shelled OLN_s or OFN_s for 24 h in normoxic or hypoxic conditions. As shown in Figure 1, confocal microscopy confirmed OLN internalization by normoxic HMEC-1 and their localization in the cytoplasm. Similar results were also obtained upon culturing HMEC-1 cells with OLN_s in hypoxic conditions and with OFN_s both in normoxic or hypoxic conditions (data not shown).

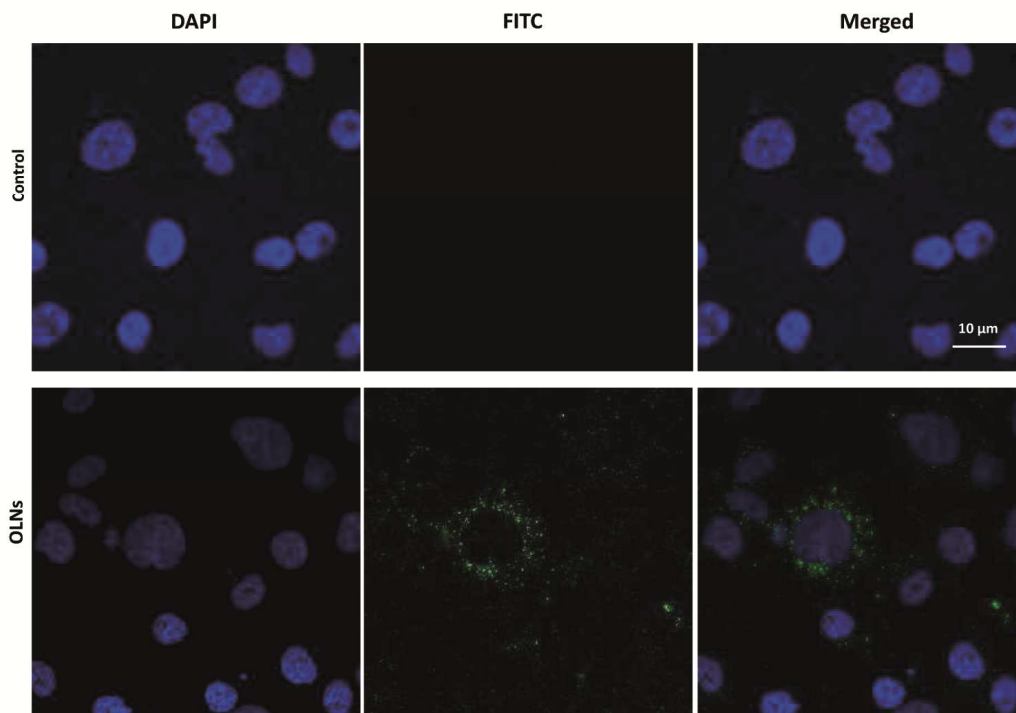


FIGURE 1. OLN internalization by human dermal microvascular endothelial cells. HMEC-1 (10^5 cells/0.5 ml MCDB 131 medium) were left untreated (upper panels) or treated with 10% v/v FITC-labeled OLN (lower panels) for 24 h in normoxia (20 % O_2). After DAPI staining, cells were checked by confocal microscopy. Results are shown as representative images from three independent experiments. Left panels: cell nuclei after DAPI staining. Central panels: FITC-labeled OLN. Right panels: merged images. Magnification: 63X.

Effects of hypoxia and OLN on HMEC-1 viability

After 24 h-incubation of HMEC-1 with or without 10% v/v OSS, OLN or OFN, both in normoxic (20% O_2) and hypoxic (1% O_2) conditions, cytotoxicity and cell viability were analyzed through LDH and MTT assays, respectively (Figure 2). As shown in Panel 2A, OSS, OLN or OFN were not toxic to HMEC-1 both in normoxic (20% O_2) and hypoxic

(1% O₂) conditions. As shown in Panel 2B, hypoxia *per se* determined an apparent reduction of the metabolic activity of HMEC-1, however such an effect was not statistically significant and in any case was fully counteracted by OLN.

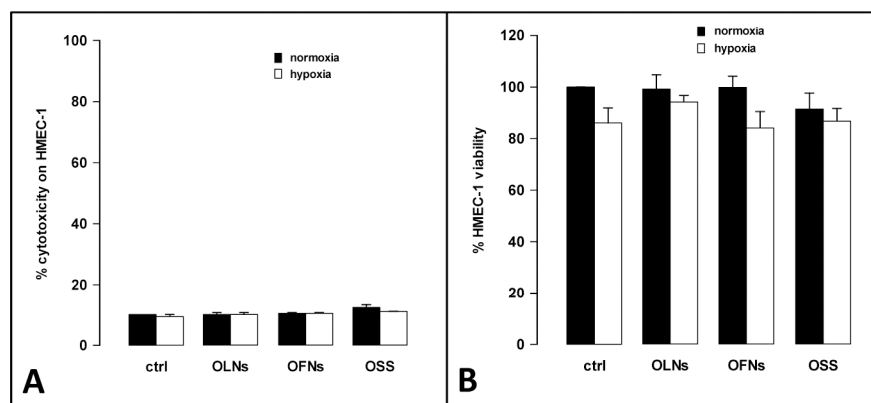
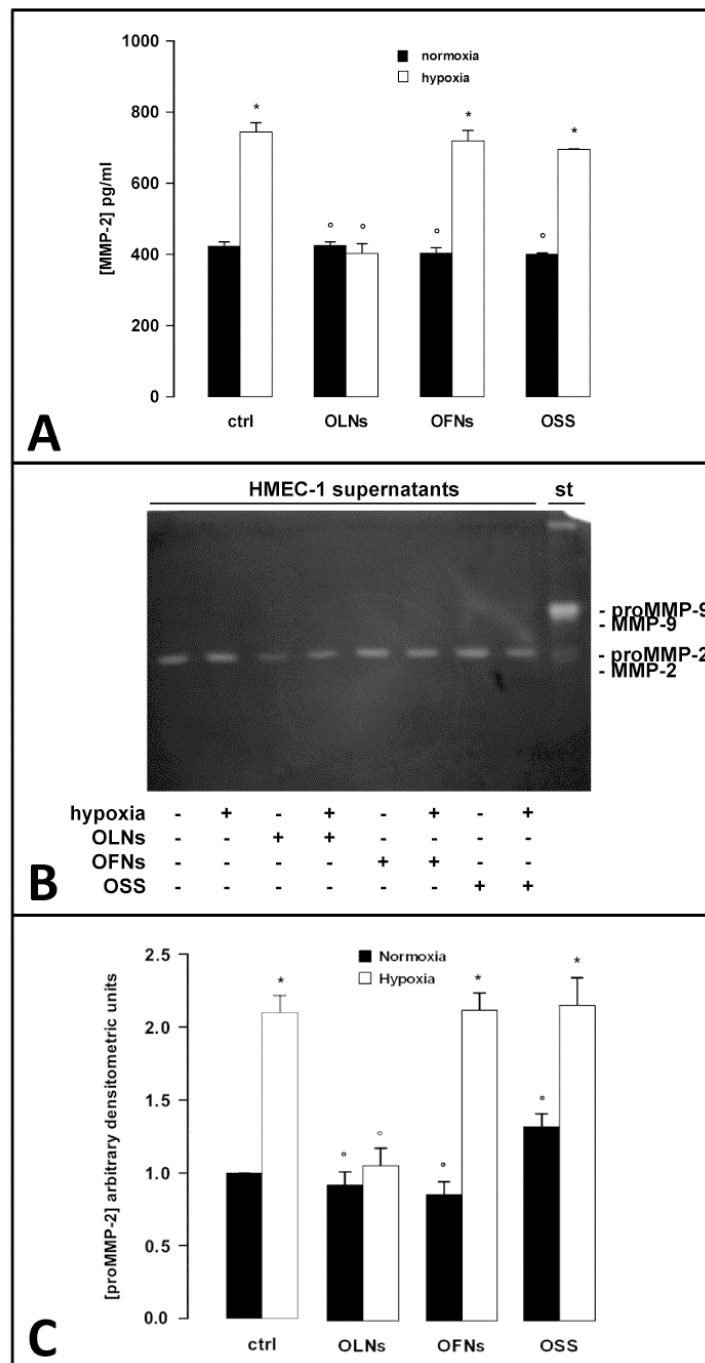


FIGURE 2. Hypoxia and OLN effects on human dermal microvascular endothelial cell viability. HMEC-1 (10^5 cells/0.5 ml MCDB 131 medium) were left untreated or treated with 10% v/v OLN, OFN or OSS for 24 h in normoxia (20% O₂, black bars) or hypoxia (1% O₂, white bars). After collection of cell supernatants and lysates, the percentage of cytotoxicity was measured by the release of LDH (panel A), whereas the percentage of cell viability was measured with the MTT assay (panel B). The results are the means+SEM from three independent experiments. Using the ANOVA test, no significant differences between normoxic or hypoxic control cells or between OLN-treated and untreated cells were observed (both panels).

374 *Hypoxia and OLN effects on gelatinase secretion by human dermal microvascular*
375 *endothelial cells*

376 After 24 h-incubation of HMEC-1 with or without 10% v/v OSS, OLN or OFNs, both in
377 normoxic (20% O₂) and hypoxic (1% O₂) conditions, the secretion of gelatinases (MMP-2
378 and MMP-9) into cell supernatants was evaluated by ELISA as well as by gelatin
379 zymography coupled to densitometry. The results are shown in Figure 3. Untreated normoxic
380 HMEC-1 constitutively secreted ~400 pg/ml of MMP-2 (Panel A). Notably, HMEC-1 only
381 secreted the 72 kDa latent form of MMP-2 (proMMP-2), whereas the 63 kDa active form was
382 not detected in the cell supernatants (Panels B-C). On the contrary, neither ELISA (not
383 shown) nor gelatin zymography analyses detected any MMP-9 protein amounts in endothelial
384 cell supernatants. Hypoxia significantly altered MMP-2 secretion by almost doubling
385 proMMP-2 levels in HMEC-1 supernatants. OLN – but not OFNs or OSS – fully reversed
386 the effects of hypoxia, restoring a normoxia-like secretion of proMMP-2.

387



388

389

390

FIGURE 3. Effects of hypoxia and OLN on MMP-2 secretion by human dermal microvascular endothelial cells. HMEC-1 (10^5 cells/0.5 ml MCDB 131 medium) were left

untreated or treated with 10% v/v OLN_s, OFN_s or OSS for 24 h in normoxia (20% O₂; panels A and C: black bars; panel B: odd lanes) or hypoxia (1% O₂; panels A and C: white bars; panel B: even lanes). After collection of cell supernatants, MMP-2 protein levels were quantified by ELISA (panel A), whereas MMP-2 latent/active forms were analyzed by gelatin zymography (panel B) and subsequent densitometry (panel C). For gelatin zymography, recombinant human proMMP-9 (92 kDa) was employed as a standard marker (st). Results are shown as means+SEM (panels A and C) or as a representative gel (panel B) from three independent experiments. ELISA and densitometric data were also evaluated for significance by ANOVA: * vs normoxic control cells: $p<0.0001$ (panel A), $p<0.0001$ (panel C); ° vs hypoxic control cells: $p<0.0001$ (panel A), $p<0.0001$ (panel C).

Hypoxia and OLN effects on TIMP secretion by human dermal microvascular endothelial cells and MMP-2/TIMP-2 balances

HMEC-1 were incubated for 24 h with or without 10% v/v OSS, OLN_s or OFN_s, both in normoxic (20% O₂) and hypoxic (1% O₂) conditions. Thereafter, the secretion of TIMP-1 and TIMP-2 was evaluated by ELISA. As shown in Figure 4, normoxic untreated HMEC-1 constitutively released ~2.2 ng/ml TIMP-1 and ~1.6 ng/ml TIMP-2. Hypoxia significantly lowered by almost 20% the secreted levels of TIMP-1 while TIMP-2 production was not affected. OLN_s – but not OFN_s and OSS - completely abrogated the effects of hypoxia, restoring physiological TIMP-1 amounts also in hypoxic culturing conditions.

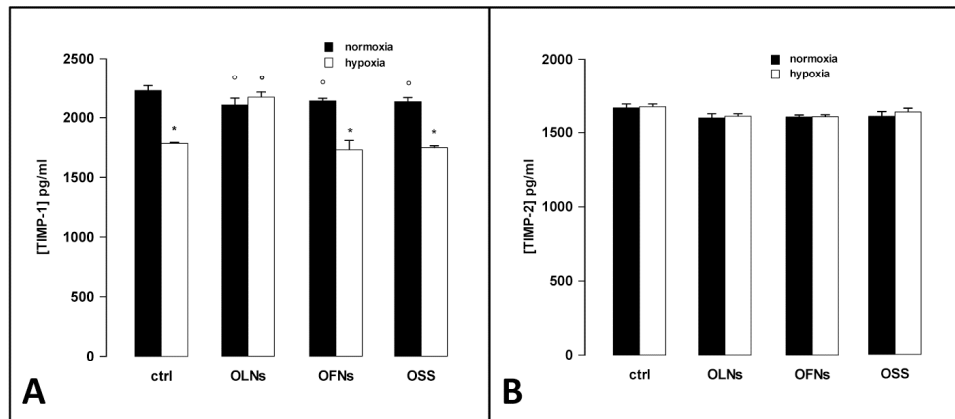


FIGURE 4. Effects of hypoxia and OLN treatments on protein levels of gelatinase inhibitors (TIMP-1 and TIMP-2) secreted by human dermal microvascular endothelial cells. HMEC-1 (10^5 cells/0.5 ml MCDB 131 medium) were left untreated or treated with 10% v/v OLN, OFN or OSS for 24 h in normoxia (20% O_2 ; black bars, both panels) or hypoxia (1% O_2 ; white bars, both panels). After collection of cell supernatants, TIMP-1 (panel A) and TIMP-2 (panel B) protein levels were quantified by ELISA. Results are shown as means+SEM from three independent experiments. Data were also evaluated for significance by ANOVA: * vs normoxic control cells: $p < 0.0001$ (panel A) and p not significant (panel B); ° vs hypoxic control cells: $p < 0.0001$ (panel A) and p not significant (panel B).

Consequently, the balance between MMP-2 and its inhibitor was calculated. As shown in Figure 5, hypoxia significantly affected MMP-2/TIMP-2 stoichiometric ratio, which was almost doubled with respect to cells cultured in normoxic conditions. OLN – but not OFN

or OSS – effectively counteracted the effects of hypoxia, restoring the MMP-2/TIMP-2 ratio to a value similar to that observed in normoxia.

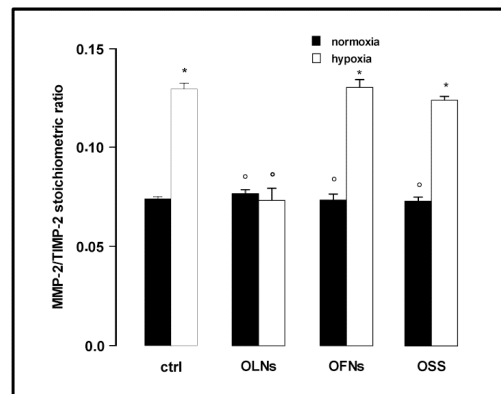


FIGURE 5. Effects of hypoxia and OLN on MMP-2/TIMP-2 balances upon secretion by dermal microvascular endothelial cells. MMP-2/TIMP-2 stoichiometric ratio was calculated from the ELISA data (see Figures 3-4). Results are shown as means+SEM from three independent experiments. Data were also evaluated for significance by ANOVA: * vs normoxic control cells: $p < 0.0001$; ° vs hypoxic control cells: $p < 0.0001$.

Effects of hypoxia and OLN on migration and wound healing abilities of human dermal microvascular endothelial cells

The ability of HMEC-1 to spontaneously migrate was investigated through an *in vitro* wound healing assay. As shown in Figure 6, hypoxic HMEC-1 displayed a lower ability to migrate

compared to normoxic cells. However, the migration ability of hypoxic HMEC-1 was significantly increased in the presence of OLN. Interestingly, OLN effects were not reproduced by OFNs, suggesting a peculiar role for oxygen released from the core of OLN.

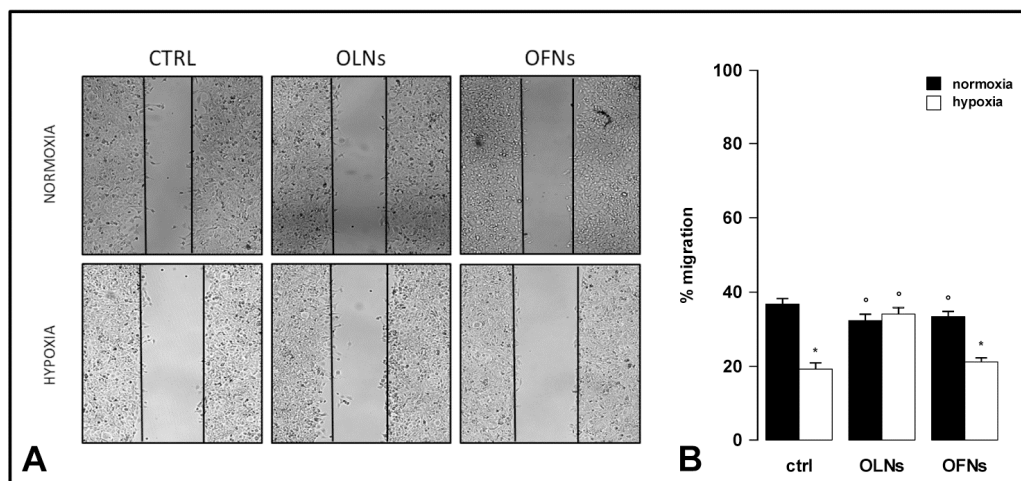


FIGURE 6. Effects of hypoxia and OLN on migration and wound healing abilities of human microvascular dermal endothelial cells. HMEC-1 were seeded in two confluent monolayers, divided by a space (scratch) of 500 μ m, and incubated for 8 h in normoxia (20% O₂) or hypoxia (1% O₂) with/without 10% v/v OLN or OFN. Thereafter, scratch lengths were measured. A: representative images. B: means \pm SEM of scratch lengths. Results are from three independent experiments performed in duplicates. Data were also evaluated for significance by ANOVA: * vs normoxic untreated cells: $p < 0.001$; ° vs hypoxic untreated cells: $p < 0.001$.

Effects of hypoxia and OLN on abilities of human dermal microvascular endothelial cells to invade collagen matrix and form microvessel-like structures

The ability of HMEC-1 to invade a collagen matrix and form microvessel-like structures was investigated through an *in vitro* invasion assay. As shown in Figure 7, hypoxic HMEC-1 displayed a lower ability to invade matrix and organize in microvessel-like structures compared to normoxic cells. However, the invasion ability (i.e. the number of crosses) of hypoxic HMEC-1 was significantly increased in the presence of OLN.

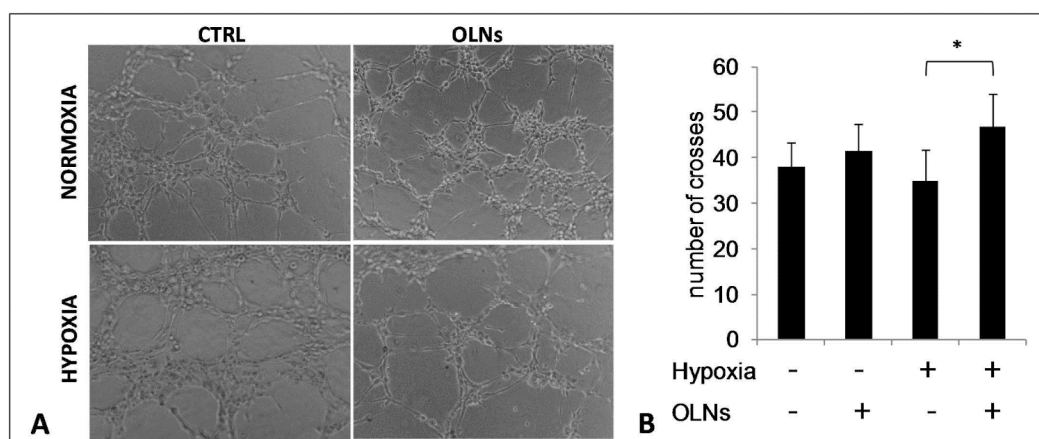


FIGURE 7. Effects of hypoxia and OLN on matrix invasion ability of human microvascular dermal endothelial cells. HMEC-1 (1×10^5 cells/0.5 ml MCDB 131 medium) were seeded on a Cultrex matrix and incubated for 2 h in normoxia (20% O₂) or hypoxia (1% O₂) with/without 10% v/v OLN. Thereafter, microvessel-like structures were checked by optical microscopy and the number of crosses between two microvessel-like structures was counted in five fields. A: representative images. B: means+SEM of numbers of crosses.

467 Results are from four independent experiments. Data were also evaluated for significance by

468 Student's *t* test: * vs hypoxic untreated cells: $p < 0.05$.

469

Discussion

During healing processes, the balance between pro- and anti-angiogenic factors determining specific endothelial cell behavior and vessel organization must be spatially and temporally controlled. Among these factors, MMPs appear as pivotal molecules. These evolutionarily conserved and tightly regulated zinc-dependent proteases are expressed either in a constitutive or inducible manner by a broad spectrum of specialized cells, including endothelial cells [Vandenbroucke et al., 2014]. Released as latent zymogens, activated locally by other proteases and inhibited in a 1:1 stoichiometric ratio by their secreted endogenous inhibitors (TIMPs) [Brew & Nagase, 2010], MMPs not only process all the components of the basement membrane and the ECM, but can also cleave cytokines, chemokines, growth factors, enzymes, and membrane-bound proteins, thus promoting their activation, inhibition, degradation or shedding [Cauwe et al., 2007]. As such, they play essential roles in cell survival, proliferation, migration, invasion, hemostasis and inflammation within the cellular milieu of the wound [Gill & Parks, 2008].

A long-lasting hypoxic environment represents a critical feature of chronic wounds [4-5]. However, the effects of hypoxia on the phenotype and the behavior of the cellular environment of the wound can be dramatically different depending on the considered cell type (monocytes, keratinocytes, endothelial cells, fibroblasts etc). To complement previous data on hypoxia-dependent dysregulation of MMP/TIMP balances in human monocytes [Gulino et al., 2015] and keratinocytes [Khadjavi et al., 2015], the present *in vitro* study aimed at investigating the effects of hypoxia on the pro-angiogenic phenotype and the wound healing abilities of human dermal microvascular endothelial cells. Furthermore, innovative and nonconventional dextran-shelled/DFP-cored OLNPs were challenged for their potential abilities to counteract the effects of hypoxia.

495 Normoxic HMEC-1 constitutively secreted MMP-2, TIMP-1, and TIMP-2 proteins while
496 MMP-9 was not observed. In particular, cells were found to constitutively release only the
497 latent 72 kDa form of MMP-2, whereas its 62 kDa activated form was not detected. These
498 results are in line with previous reports on endothelial cells from both micro- and macro-
499 vascular vessels [Hanemaaijer et al., 1993; Ben-Yosef et al., 2002; Ben-Yosef et al., 2005;
500 Bertl et al., 2006]. Exposure of endothelial cells to prolonged hypoxia led to enhanced MMP-
501 2 and diminished TIMP-2 protein levels in cell supernatants, whereas TIMP-1 production
502 was not altered. The increase of MMP-2 resulted in elevated zymogen secretion but not in the
503 active form of the enzyme. Notably, latent MMP-2 undergoes activation mainly through
504 interactions with membrane-bound MT1-MMP and the $\alpha_v\beta_3$ integrin [Deryugina et al., 2001;
505 Hofmann et al., 2008]. Additionally, low levels of TIMP-2, the main MMP-2 inhibitor,
506 participate in MT1-MMP-mediated activation of MMP-2, while high levels of TIMP-2 can
507 block MMP-2 activation [Brew & Nagase, 2010]. Interestingly, hypoxia-dependent down-
508 regulation of MT1-MMP expression was previously reported for human endothelial cells
509 [Ben-Yosef et al., 2002]. This might justify the absence of the active 62 kDa form of MMP-2
510 in the present hypoxic model.

511 HMEC-1 were also challenged under hypoxic conditions for their ability to migrate, invade
512 the ECM and form tube-like structures. Indeed, ECM structure and composition provides a
513 scaffold and signals for cell adhesion and migration during tissue restoration [Li et al., 2005].
514 ECM effect on angiogenesis appears highly variable over time, strictly depending on protein
515 constituents, protease actions, and ECM ability to sequester growth factors and bioactive
516 molecular fragments [Wells et al., 2015]. Significantly, MMP-mediated degradation of ECM
517 can promote endothelial cell migration through exposure of pro-migratory matrix molecule
518 binding sites [Pepper, 2001; Hangai et al., 2002]. However, in the present work hypoxic
519 HMEC-1 displayed lower abilities to migrate and promote wound healing, as well as to

invade a collagen matrix and organize in tube-like structures compared to normoxic cells, despite increased MMP-2 levels. Interestingly, similar results were obtained by Ben-Yosef and colleagues in a previous work using endothelial cells from large caliber vessels, where hypoxia led concurrently to an increase in proMMP-2 secretion and to a significant reduction in the number of tube-like structures spontaneously formed in the culture [Ben-Yosef et al., 2005]. Since specific MMP-2 inhibitors did not restore the normal tube-like formation, the authors concluded that hypoxia-induced anti-angiogenic effects responsible for the observed reduction in tube-like formation were not mediated by MMP-2. Consistently, in another *in vitro* model, tube-like formation in human microvascular endothelial cells was shown to depend directly on membrane-bound MT1-MMP and not on secreted MMPs such as MMP-2 [Koike et al, 2002]. Therefore, the compromised migration and invasion abilities of HMEC-1 highlighted here might be secondary to hypoxia-induced reduction of MT1-MMP, previously reported for endothelial cells [Ben-Yosef et al., 2002]. On the other hand, in chronic wounds, reduced protein levels compared to acute wounds have been described for several growth factors including FGF, EGF, PDGF, VEGF, and TGF- β , secondary to trapping by ECM molecules or excessive degradation by MMPs [Greaves et al., 2013]. Importantly, many of these growth factors are MMP-2 substrates, including TGF- β , released after decorin cleavage [Cauwe et al., 2009; Imai et al., 1997].

Once ascertained that hypoxia hampers HMEC-1 pro-angiogenic phenotype and behavior by increasing MMP-2/TIMP-2 stoichiometric ratio and reducing cell migration and ECM invasion abilities, new dextran-shelled OLN [Prato et al., 2015] were challenged for their therapeutic potential to counteract the effects of hypoxia. The core structure of these innovative and nonconventional gas nanocarriers is constituted by DFP, a stable and biologically inert liquid fluorocarbon which carries molecular oxygen without actually binding it, thus favoring gas exchange [Cote et al., 2008]. On the other hand, OLN shell is

545 constituted by dextran, a well-known polysaccharide classified as class 4 (low-toxicity)
546 substance [Bos et al., 2005]. OLN_s are able to release significant amounts of oxygen into
547 hypoxic environments in a time-sustained manner, opposite to OSS, which releases oxygen
548 only transiently, and to OFN_s, not releasing oxygen at all [Prato et al., 2015]. All sterile
549 nanodroplet preparations employed here displayed spherical shapes, nanometric sizes,
550 negative charges, high stability over time, and good oxygen-storing and -releasing abilities, in
551 accordance with literature data [Prato et al., 2015].

552 OLN_s were internalized by HMEC-1 into the cytoplasmic region, not entering the nuclei.
553 This evidence complements previous data on the uptake of OLN_s by other eukaryotic cells,
554 including human keratinocytes [Prato et al., 2015, Khadjavi et al., 2015] and monocytes
555 [Gulino et al., 2015]. OLN_s did not display cytotoxic effects on HMEC-1. Even more so, OLN_s
556 fully abrogated hypoxia-dependent dysregulating effects on proteolytic activity, restoring
557 normoxia-like balances between MMP-2 and TIMP-1/2 and improving migration and ECM
558 invasion abilities. These effects were specifically dependent on time-sustained oxygen release
559 from the inner core of OLN_s, since they were not reproduced after treatment with OFN_s or
560 OSS. These results are in full agreement with those obtained from parallel works with
561 dextran-shelled OLN_s, able to restore normoxia-like MMP-9/TIMP-1 ratio in hypoxic human
562 monocytes [Gulino et al., 2015], and chitosan-shelled OLN_s, effective in abrogating hypoxia-
563 dependent dysregulation of balances between gelatinases and their inhibitors in human
564 keratinocytes [Khadjavi et al., 2015]. Therefore, the findings proposed here appear extremely
565 relevant to reach a global vision of the pro-angiogenic phenotype of the chronic wound, since
566 endothelial cells play relevant roles during healing processes in concert with both monocytes
567 and keratinocytes [Eming et al., 2014].

568 In conclusion, the present work shows that prolonged hypoxia significantly alters the
569 phenotype and behavior of human dermal microvascular endothelium, enhancing MMP-2 and

reducing TIMP-1 secretion, and compromising cell abilities to migrate, promote wound healing, invade the ECM and form tube-like structures. These findings enlarge the available knowledge on the effects of hypoxia on the pro-angiogenic profile of single cell populations actively involved in wound healing processes, thus helping to better understand the dynamics occurring at the milieu of the hypoxic chronic wound. Intriguingly, dextran-shelled/DFP-cored OLN_s proved effective in counteracting hypoxia, reestablishing normoxia-like pro-angiogenic features in hypoxic microvascular endothelial cells. As such, these results support the proposal that OLN_s should be tested as innovative, nonconventional, cost-effective, and nontoxic adjuvant therapeutic tools for chronic wound treatment, in order to promote or accelerate tissue repair and the regeneration processes. Based on the present *in vitro* evidence, future preclinical studies to translate OLN technology to clinical practice are envisaged.

Acknowledgements

We gratefully acknowledge the Compagnia di San Paolo (Ateneo-San Paolo 2011 ORTO11CE8R grant to CG and MP) and Università degli Studi di Torino (ex-60% 2013 intramural funds to GG and MP) for funding support to this work. MP holds a professorship granted by Università degli Studi di Torino and Azienda Sanitaria Locale-19 (ASL-19). AK and MP are funded by a partnership grant from the European Community and the Italian Ministry of Instruction, University, and Research (CHIC grant no. 600841). NB and SDA research is supported by the Italian Ministry of Instruction, University, and Research (PRIN 2013 grant). The authors are sincerely grateful to Adriano Troia for his suggestions on nanodroplet manufacturing, to Donatella Taramelli for her comments on the manuscript, and to Ghislain Opdenakker and Philippe Van den Steen for kindly giving recombinant human proMMP-9. The authors have no conflicting financial interests.

596 **List of Abbreviations**

597

598 ANOVA, analysis of variance; DAPI, 4',6-diamidino-2-phenylindole; DFP, 2H,3H-
599 decafluoropentane; MTT, 3-(4,5-dimethylthiazol-2-yl)-2,5-diphenyltetrazolium bromide;
600 ECM, extracellular matrix; FITC, fluorescein isothiocyanate; LDH, lactate dehydrogenase;
601 MMP, matrix metalloproteinase; OFN, oxygen-free nanodroplet; OLN, oxygen-loaded
602 nanodroplet; OSS, oxygen-saturated solution; PBS, phosphate-buffered saline; PFP,
603 perfluoropentane; TIMP, tissue inhibitor of metalloproteinase; US, ultrasound; UV,
604 ultraviolet.

605

References

- Ades, E.W., Candal, F.J., Swerlick, R.A., George, V.G., Summers, S., Bosse, D.C., Lawley, T.J. HMEC-1: establishment of an immortalized human microvascular endothelial cell line. *J Invest Dermatol.* 1992;99, :683-690.
- Ben-Yosef, Y., Lahat, N., Shapiro, S., Bitterman, H., Miller, A. Regulation of endothelial matrix metalloproteinase-2 by hypoxia/reoxygenation. *Circ Res.* 2002;90, :784-791.
- Ben-Yosef, Y., Miller, A., Shapiro, S., Lahat, N. Hypoxia of endothelial cells leads to MMP-2-dependent survival and death. *Am J Physiol Cell Physiol.* 2005;289, :C1321-1331.
- Bertl, E., Bartsch, H., Gerhäuser, C. Inhibition of angiogenesis and endothelial cell functions are novel sulforaphane-mediated mechanisms in chemoprevention. *Mol Cancer Ther.* 2006;5, :575-585.
- Bos, G.W., Hennink, W.E., Brouwer, L.A., den Otter, W., Veldhuis, F.J., Van Nostrum, C.F., Van Luyn, M.J. Tissue reactions of in situ formed dextran hydrogels crosslinked by stereocomplex formation after subcutaneous implantation in rats. *Biomaterials.* 2005;26, :3901–3909.
- Brew, K., Nagase, H. The tissue inhibitors of metalloproteinases (TIMPs): an ancient family with structural and functional diversity. *Biochim Biophys Acta.* 2010;1803, :55-71.
- Cabrales, P., Intaglietta, M. Blood substitutes: evolution from noncarrying to oxygen- and gas-carrying fluids. *ASAIO J.* 2013;59, : 337-354.
- Castilla, D.M., Liu, Z.J., Velazquez, O.C. Oxygen: Implications for Wound Healing. *Adv Wound Care (New Rochelle).* 2012; 1, :225-30.
- Cauwe, B., Van den Steen, P.E., Opdenakker, G. The biochemical, biological, and pathological kaleidoscope of cell surface substrates processed by matrix metalloproteinases. *Crit Rev Biochem Mol Biol.* 2007;42, :113-185.
- Cavalli, R., Bisazza, A., Rolfo, A., Balbis, S., Madonnaripa, D., Caniggia, I., Guiot, C. Ultrasound-mediated oxygen delivery from chitosan nanobubbles. *Int J Pharm.* 2009;378, :215-217.
- Cavalli, R., Bisazza, A., Giustetto, P., Civra, A., Lembo, D., Trotta, G., et al. Preparation and characterization of dextran nanobubbles for oxygen delivery. *Int J Pharm* 2009;381, :160-165.
- Cote, M., Rogueda, P.G., Griffiths, P.C. Effect of molecular weight and end-group nature on the solubility of ethylene oxide oligomers in 2H, 3H-decafluoropentane and its fully fluorinated analogue, perfluoropentane. *J Pharm Pharmacol.* 2008;60, :593-599.
- D'Alessandro, S., Basilico, N., Prato, M. Effects of Plasmodium falciparum-infected erythrocytes on matrix metalloproteinase-9 regulation in human microvascular endothelial cells. *Asian Pac J Trop Med.* 2013;6, :195-199.

Deryugina, E.I., Ratnikov, B., Monosov, E., Postnova, T.I., DiScipio, R., Smith, J.W., Strongin, A.Y. MT1-MMP initiates activation of pro-MMP-2 and integrin $\alpha_v\beta_3$ promotes maturation of MMP-2 in breast carcinoma cells. *Exp Cell Res.* 2001;263, :209–223.

Diegelmann, R.F., Evans, M.C. Wound healing: an overview of acute, fibrotic and delayed healing. *Front Biosci.* 2004; 9, : 283-289.

Eming, S.A., Martin, P., Tomic-Canic, M. Wound repair and regeneration: mechanisms, signaling, and translation. *Sci Transl Med.* 2014; 6, :265sr6.

Gill, S.E., Parks, W.C. Metalloproteinases and their inhibitors: regulators of wound healing. *Int J Biochem Cell Biol.* 2008;40, :1334-1347.

Greaves, N.S., Ashcroft, K.J., Baguneid, M., Bayat, A. Current understanding of molecular and cellular mechanisms in fibroplasia and angiogenesis during acute wound healing. *J Dermatol Sci.* 2013; 72, : 206-217.

Gulino, G.R., Magonetto, C., Khadjavi, A., Panariti, A., Rivolta, I., Soster, M., et al. Oxygen-loaded nanodroplets effectively abrogate hypoxia dysregulating effects on secretion of matrix metalloproteinase-9 and tissue inhibitor of metalloproteinase-1 by human monocytes. *Mediators of Inflammation*, 2015;2015, :964838.

Hanemaaijer, R., Koolwijk, P., le Clercq, L., de Vree, W.J., van Hinsbergh, V.W. Regulation of matrix metalloproteinase expression in human vein and microvascular endothelial cells. Effects of tumour necrosis factor alpha, interleukin 1 and phorbol ester. *Biochem J.* 1993;296, :803-809.

Hangai, M., Kitaya, N., Xu, J., Chan, C.K., Kim, J.J., Werb, Z., et al. Matrix metalloproteinase-9-dependent exposure of a cryptic migratory control site in collagen is required before retinal angiogenesis. *Am J Pathol.* 2002;161, :1429-1437.

Hofmann, U.B., Westphal, J.R., Van Kraats, A.A., Ruiter, D.J., Van Muijen, G.N.P. Expression of integrin $\alpha_v\beta_3$ correlates with activation of membrane-type matrix metalloproteinase-1 (MT1-MMP) and matrix metalloproteinase-2 (MMP-2) in human melanoma cells in vitro and in vivo. *Int J Cancer.* 2000;87, :12–19.

Imai, K., Hiramatsu, A., Fukushima, D., Pierschbacher, M.D., Okada, Y. Degradation of decorin by matrix metalloproteinases: identification of the cleavage sites, kinetic analyses and transforming growth factor-beta1 release. *Biochem J.* 1997;322, : 809-814.

Khadjavi, A., Magonetto, C., Panariti, A., Argenziano, M., Gulino, G.R., Rivolta, I., et al. Chitosan-shelled oxygen-loaded nanodroplets abrogate hypoxia dysregulation of human keratinocyte gelatinases and inhibitors: new insights for chronic wound healing. *Toxicol Appl Pharmacol.* 205; 286, :198-206.

Koike, T., Vernon, R.B., Hamner, M.A., Sadoun, E., Reed, M.J. MT1-MMP, but not secreted MMPs, influences the migration of human microvascular endothelial cells in 3-dimensional collagen gels. *J Cell Biochem.* 2002;86, :748–758.

Li, S., Huang, N.F., Hsu, S. Mechanotransduction in endothelial cell migration. *J Cell Biochem.* 2005;96, :1110-1126.

Magnetto, C., Prato, M., Khadjavi, A., Giribaldi, G., Fenoglio, I., Jose, J., et al. Ultrasound-activated decafluoropentane-cored and chitosan-shelled nanodroplets for oxygen delivery to hypoxic cutaneous tissues. *RSC Adv.* 2014;4, :38433-38441.

Pepper, M.S. Extracellular proteolysis and angiogenesis. *Thromb Haemost.* 2001;86, :346-355.

Prato, M., D'Alessandro, S., Van den Steen, P.E., Opdenakker, G., Arese, P., Taramelli, D., Basilico, N. Natural haemozoin modulates matrix metalloproteinases and induces morphological changes in human microvascular endothelium. *Cell Microbiol.* 2011;13, :1275-1285.

Prato, M., Magnetto, C., Jose, J., Khadjavi, A., Cavallo, F., Quaglino, E., et al. 2H,3H-decafluoropentane-based nanodroplets: new perspectives for oxygen delivery to hypoxic cutaneous tissues. *Plos One.* 2015;10, :e0119769.

Schroeter, A., Engelbrecht, T., Neubert, R.H.H., Goebel, A.S.B. New Nanosized Technologies for Dermal and Transdermal Drug Delivery. A Review. *J Biomed Nanotechnol.* 2010 ;6, :511–528.

Sen, C.K. Wound healing essentials: let there be oxygen. *Wound Repair Regen.* 2009; 17, :1-18.

Vandenbroucke, R.E., Libert, C. Is there new hope for therapeutic matrix metalloproteinase inhibition? *Nat Rev Drug Discov.* 2014,13, :904-927.

Wells, J.M., Gaggari, A., Blalock, J.E. MMP generated matrikines. *Matrix Biol.* 2015;44-46C, :122-129.